

Inclusive Scattering of Polarized Electrons on Polarized ^3He : Effects of Final State Interaction and the Magnetic Form Factor of the Neutron

S. Ishikawa

Department of Physics, Hosei University, Fujimi 2-17-1, Chiyoda, Tokyo 102, Japan

J. Golak and H. Witała

Institute of Physics, Jagellonian University, PL-30059 Cracow, Poland

H. Kamada*, W. Glöckle and D. Hüber†

Institut für Theoretische Physik II, Ruhr-Universität Bochum, D-44780 Bochum, Germany

(September 6, 2018)

Abstract

Effects of final state interaction on asymmetries in inclusive scattering of polarized electrons on polarized ^3He are investigated using consistent ^3He bound state wave function and 3N continuum scattering states. Significant effects are found, which influence the extraction of the magnetic neutron form factor from $A_{T'}$. The enhancement found experimentally for $A_{TL'}$ near the 3N breakup threshold, which could not be explained in calculations carried through in plane wave impulse approximation up to now, occurs now also in

*present address: Institut für Kernphysik, Fachbereich 5 der Technischen Hochschule Darmstadt, D-64289 Darmstadt, Germany

†present address: Los Alamos National Laboratory, Theoretical Division, Los Alamos, NM 87545

theory if the full final state interaction is included.

13.40.Gp, 13.60.Hb, 21.45.+v, 24.70.+s, 25.30.Fj

I. INTRODUCTION

The electromagnetic form factor of the nucleons are of fundamental interest in nuclear and particle physics. While the proton form factors have been determined from elastic electron-proton scattering over a wide range of momentum transfers with good accuracy [1], this is not the case for the neutron, since no free neutron targets exist. One is therefore forced to extract information on the neutron from electron scattering on light nuclei. Obviously ambiguities arising from nuclear structure and reaction mechanisms should be minimized. So far mainly the deuteron has been used as a target [2]. The ^3He nucleus has also attracted much attention as an ideal target [3,4]. If one assumes that the ^3He wave function is spatially symmetric (antisymmetric in spin-isospin space), then the spins of the two protons are coupled to zero and the spin of ^3He is carried by the neutron alone. Under this simplifying assumption a polarised ^3He nucleus can be considered to be a polarised neutron. Now this picture of the ^3He wave function, the so-called principal S-state approximation, is valid to about 92 % with respect to its norm. (This refers to Bonn B potential [19], which we use in this article) Motivated by that attractive feature, recently several experiments have been performed, where longitudinally polarized electrons with helicities $h(=\pm 1)$ have been inclusively scattered on polarized ^3He targets [5–9]. The aim was to measure the asymmetries

$$A = \frac{\sigma(h = +1) - \sigma(h = -1)}{\sigma(h = +1) + \sigma(h = -1)}, \quad (1)$$

depending on the spin direction of ^3He . These asymmetries are expected to be sensitive to the electromagnetic form factors of the neutron. The data have been analysed so far in plane wave impulse approximation [10,11] and based on a single nucleon current operator. That approximation neglects the interaction between the nucleon which absorbed the photon and the two other nucleons.

It is the aim of this investigation to remove that theoretical uncertainty and to treat the ^3He bound state wave function and the 3N continuum representing the final 3N scattering state on an equal footing, using exact solutions of three-body Faddeev equations based on

realistic NN forces. Our theoretical formalism is described in section II and our results in comparison to the data in section III. A Summary is given in section IV.

II. THEORY

In recent articles [12–16] we studied elastic and inelastic electron scattering on ${}^3\text{He}$ corresponding to unpolarized experiments. So far our dynamical picture is: a nonrelativistic framework, a single nucleon current operator and the exact treatment of realistic NN forces among the three nucleons. For the relatively low momentum transfers considered up to now that picture was quite successful and the final state interaction (FSI) among the three nucleons played a significant role. Now we apply that dynamical picture to the scattering of polarized electrons on polarized ${}^3\text{He}$ targets under inclusive conditions. The derivation of the corresponding cross section is known [17]. However to stay in line with the notation in our previous articles and to show its extensions we just mention the new ingredients. In the evaluation of the cross section the fixed electron polarization in the initial state leads to an additional term proportional to the helicity h on top of the usual expression for the electron tensor

$$\begin{aligned} L^{\mu\nu} &\equiv \sum_{s'} \bar{u}(k's')\gamma^\mu u(ks)(\bar{u}(k's')\gamma^\nu u(ks))^* \\ &= \frac{1}{2m^2}(k^\mu k'^\nu + k'^\mu k^\nu - g^{\mu\nu}k \cdot k' + ih\epsilon^{\mu\nu\alpha\beta}k_\alpha k'_\beta) \end{aligned} \quad (2)$$

That additional last term in Eq. (2) has been evaluated under the condition, that the electron mass m can be neglected in relation to its energy. Straightforward contraction with the hadronic tensor yields the inclusive cross section in the lab system

$$\frac{d\sigma}{d\hat{k}'dk_0} = \sigma_{Mott} [v_L R_L + v_T R_T + h(v_{T'} R_{T'} + v_{TL'} R_{TL'})] \quad (3)$$

The unprimed terms are the familiar ones for the unpolarized set up [16]. The primed terms are: kinematical factors from the electron tensor

$$v_{T'} = \sqrt{\frac{-Q^2}{\vec{Q}^2} + \tan^2 \frac{\Theta}{2}} \tan \frac{\Theta}{2} \quad (4)$$

$$v_{TL'} = \frac{1}{\sqrt{2}} \frac{Q^2}{\bar{Q}^2} \tan \frac{\Theta}{2} \quad (5)$$

and structure functions related to the hadronic tensor

$$R_{T'} = \sum_{m' \tau'} \int df' \delta(M + \omega - P'_0) (|N_1|^2 - |N_{-1}|^2) \quad (6)$$

$$R_{TL'} = - \sum_{m' \tau'} \int df' \delta(M + \omega - P'_0) 2\text{Re} [N_0 (N_1 + N_{-1})^*] \quad (7)$$

Here $Q = (\omega, \vec{Q})$ is the four momentum of the photon, Θ the electron scattering angle, M the target mass and P'_0 the total energy of the final state. The summation over all spin and isospin magnetic quantum numbers and momenta in the final state is indicated by m' , τ' and df' . The nuclear matrix elements N_0 and $N_{\pm 1}$ are

$$N_0 = \langle \Psi_{f'm'\tau'}^{(-)} | \rho(\vec{Q}) | \Psi_{3\text{He}} \rangle \quad (8)$$

$$N_{\pm 1} = \langle \Psi_{f'm'\tau'}^{(-)} | j_{\pm 1}(\vec{Q}) | \Psi_{3\text{He}} \rangle, \quad (9)$$

where $|\Psi_{3\text{He}}\rangle$ is the ^3He ground state, $|\Psi_{f'm'\tau'}^{(-)}\rangle$ a 3N scattering state with the asymptotic quantum numbers $f'm'\tau'$, $\rho(\vec{Q})$ the electromagnetic hadronic density operator and $j_{\pm 1}(\vec{Q})$ the spherical components of the electromagnetic hadronic current operator. Since we use a nonrelativistic framework, the argument of the δ -function in Eqs. (6-7) is

$$\begin{aligned} M + \omega - P'_0 &= \epsilon_{3\text{He}} + \omega - \frac{\vec{Q}^2}{6m_N} - E_{f'} \\ &\equiv E - E_{f'} \end{aligned} \quad (10)$$

where $\epsilon_{3\text{He}}$ is the ^3He binding energy (negative), m_N the nucleon mass, the final total momentum $\vec{P}' = \vec{Q}$ and $E_{f'}$ the internal 3N energy related to the quantum numbers f' .

In evaluating the primed structure functions we can generalise a method proposed in [14].

Let us define

$$\mathcal{R}_{AB} \equiv \sum_{m' \tau'} \int df' \delta(E - E_{f'}) \langle \Psi_{f'm'\tau'}^{(-)} | A | \Psi_{3\text{He}} \rangle \langle \Psi_{f'm'\tau'}^{(-)} | B | \Psi_{3\text{He}} \rangle^*$$

$$\begin{aligned}
&= \sum_{m'\tau'} \int df' \langle \Psi_{3\text{He}} | B^\dagger | \Psi_{f'm'\tau'}^{(-)} \rangle \delta(E - E_{f'}) \langle \Psi_{f'm'\tau'}^{(-)} | A | \Psi_{3\text{He}} \rangle \\
&= \sum_{m'\tau'} \int df' \langle \Psi_{3\text{He}} | B^\dagger \delta(E - H) | \Psi_{f'm'\tau'}^{(-)} \rangle \langle \Psi_{f'm'\tau'}^{(-)} | A | \Psi_{3\text{He}} \rangle \\
&= \langle \Psi_{3\text{He}} | B^\dagger \delta(E - H) A | \Psi_{3\text{He}} \rangle
\end{aligned} \tag{11}$$

We introduced the 3N Hamiltonian H and used the completeness relation (the ground state does not contribute, since E lies in the 3N continuum). In our case the operators A and B are either $\rho(\vec{Q})$ or $j_\pm(\vec{Q})$.

If the operators A and B are different the method proposed in [14] to evaluate the last expression in Eq. (11) has to be generalised to

$$\begin{aligned}
\mathcal{R}_{AB} &= \frac{1}{2\pi i} \langle \Psi_{3\text{He}} | B^\dagger \frac{1}{E - i\epsilon - H} A | \Psi_{3\text{He}} \rangle - \frac{1}{2\pi i} \langle \Psi_{3\text{He}} | B^\dagger \frac{1}{E + i\epsilon - H} A | \Psi_{3\text{He}} \rangle \\
&\equiv \frac{1}{2\pi i} \langle \Psi_{3\text{He}} | B^\dagger | \Psi_A^{(-)} \rangle - \frac{1}{2\pi i} \langle \Psi_{3\text{He}} | B^\dagger | \Psi_A^{(+)} \rangle
\end{aligned} \tag{12}$$

We introduced

$$| \Psi_A^{(\pm)} \rangle \equiv \frac{1}{E \mp i\epsilon - H} A | \Psi_{3\text{He}} \rangle \tag{13}$$

Now

$$\begin{aligned}
\langle \Psi_{3\text{He}} | B^\dagger | \Psi_A^{(-)} \rangle &= \langle \Psi_A^{(-)} | B | \Psi_{3\text{He}} \rangle^* \\
&= \langle \Psi_{3\text{He}} | A^\dagger \frac{1}{E + i\epsilon - H} B | \Psi_{3\text{He}} \rangle^* \\
&\equiv \langle \Psi_{3\text{He}} | A^\dagger | \Psi_B^{(+)} \rangle^*
\end{aligned} \tag{14}$$

with

$$| \Psi_B^{(+)} \rangle = \frac{1}{E + i\epsilon - H} B | \Psi_{3\text{He}} \rangle \tag{15}$$

Therefore we get

$$\mathcal{R}_{AB} = \frac{1}{2\pi i} (\langle \Psi_{3\text{He}} | A^\dagger | \Psi_B^{(+)} \rangle^* - \langle \Psi_{3\text{He}} | B^\dagger | \Psi_A^{(+)} \rangle) \tag{16}$$

For $A = B$ we recover the old result [14]

$$\mathcal{R}_{AA} = -\frac{1}{\pi} \text{Im} \langle \Psi_{3\text{He}} | A^\dagger | \Psi_A^{(+)} \rangle \tag{17}$$

The states $|\Psi_{A,B}^{(+)}\rangle$, defined in Eqs. (13) and (15) contain all the complexity of the interaction among the three nucleons and are evaluated as in [14,16] using the Faddeev scheme.

We get

$$\Psi_C^{(+)} = G_0(1 + P)U_C \quad (18)$$

with

$$U_C = (1 + tG_0)C^{(1)}|\Psi_{3\text{He}}\rangle + tG_0PU_C \quad (19)$$

Here C is either A or B (for instance ρ or j_{\pm}) and we assumed that A or B can be decomposed as

$$C = \sum_{i=1}^3 C^{(i)}. \quad (20)$$

Further t is the NN t-matrix, G_0 the free 3N propagator and P the sum of a cyclic and anticyclic permutation of 3 objects.

The Faddeev equation (19) has been introduced and handled numerically before in [16].

Inserting Eq. (19) into Eq. (16) we get

$$\begin{aligned} \mathcal{R}_{AB} &= \frac{1}{2\pi i} \left(\langle \Psi_{3\text{He}} | A^\dagger G_0(1 + P)U_B \rangle^* - \langle \Psi_{3\text{He}} | B^\dagger G_0(1 + P)U_A \rangle \right) \\ &= \frac{3}{2\pi i} \left(\langle \Psi_{3\text{He}} | A^{(1)\dagger} G_0(1 + P)U_B \rangle^* - \langle \Psi_{3\text{He}} | B^{(1)\dagger} G_0(1 + P)U_A \rangle \right) \end{aligned} \quad (21)$$

In the last step we used Eq. (20) and the fact that the states to the left and right of A^\dagger or B^\dagger are antisymmetrical.

Regarding Eqs. (6) and (7) we see that the expressions \mathcal{R}_{AB} are either of the form \mathcal{R}_{AA} and therefore real or for $A \neq B$ one has to take the real part thereof. Thus in general we have to add the step

$$\begin{aligned} R_{AB} &= \text{Re}[\mathcal{R}_{AB}] \\ &= \frac{3}{2\pi} \text{Im} \left[\langle \Psi_{3\text{He}} | A^{(1)\dagger} G_0(1 + P)U_B \rangle^* - \langle \Psi_{3\text{He}} | B^{(1)\dagger} G_0(1 + P)U_A \rangle \right]. \end{aligned} \quad (22)$$

This applies to $R_{TL'}$ in our case.

Further considerations require a partial wave decomposition and taking the polarization of ${}^3\text{He}$ into account. We introduce our standard basis in momentum space [18]

$$|pq\alpha\rangle = |pq(ls)j(\lambda\frac{1}{2})J\mathcal{J}M(t\frac{1}{2})TM_T\rangle, \quad (23)$$

where p and q are magnitudes of Jacobi momenta and the set of discrete quantum numbers α comprises angular momenta, spins and isospins for a three-nucleon system. The ${}^3\text{He}$ state polarized in the direction θ^* , ϕ^* is

$$|\Psi_{{}^3\text{He}}m\rangle_{\theta^*\phi^*} = \sum_{m'} |\Psi_{{}^3\text{He}}m'\rangle D_{m',m}^{(1/2)}(-\phi^*, -\theta^*, 0), \quad (24)$$

where $|\Psi_{{}^3\text{He}}m\rangle$ is quantised with respect to the z -direction and the Wigner D -function occurs as

$$D_{m',m}^{(1/2)}(-\phi^*, -\theta^*, 0) = e^{-im'\phi^*} \begin{pmatrix} \cos\frac{\theta^*}{2} & -\sin\frac{\theta^*}{2} \\ \sin\frac{\theta^*}{2} & \cos\frac{\theta^*}{2} \end{pmatrix} \quad (25)$$

Using all that we get

$$\begin{aligned} \theta^*\phi^* \langle \Psi_{{}^3\text{He}}m | B^{(1)\dagger} G_0(1+P)U_A \rangle &= \sum_{\alpha} \int_0^{\infty} p^2 dp \int_0^{\infty} q^2 dq \frac{1}{E + i\epsilon - \frac{p^2}{m} - \frac{3}{4m}q^2} \\ &\sum_{m'} \sum_{m''} D_{m',m}^{(1/2)*} D_{m'',m}^{(1/2)} \langle pq\alpha | (1+P)B^{(1)} | \Psi_{{}^3\text{He}}m' \rangle^* \langle pq\alpha | U_A m'' \rangle \end{aligned} \quad (26)$$

Note that the state $|U_A\rangle$ depends on the magnetic quantum number m of ${}^3\text{He}$ through the driving term in Eq.(19).

Let us illustrate how the dependence on the magnetic quantum number m of the ${}^3\text{He}$ polarization enters into the four structure functions of Eq. (3) in two examples. The remaining ones are worked out in the Appendix. The longitudinal structure function R_L has the form

$$\begin{aligned} R_L &= -\frac{3}{\pi} \text{Im} \left[\langle \Psi_{{}^3\text{He}} | \rho^{(1)\dagger} G_0(1+P)U_{\rho} \rangle \right] \\ &= -\frac{3}{\pi} \text{Im} \left[\int \frac{1}{E + i\epsilon - \frac{p^2}{m} - \frac{3}{4m}q^2} \sum_{m'} \sum_{m''} \right. \\ &\quad \left. D_{m',m}^{(1/2)*} D_{m'',m}^{(1/2)} \langle pq\alpha | (1+P)\rho^{(1)} | \Psi_{{}^3\text{He}} m' \rangle^* \langle pq\alpha | U_{\rho} m'' \rangle \right] \end{aligned} \quad (27)$$

The sums in $\sum_{\mathcal{J}M}$ include the summation over the magnetic quantum number M of the total 3N angular momentum \mathcal{J} . We indicate that dependence on $\mathcal{J}M$ now explicitly and consider the expression

$$\sum_M \sum_{m'} \sum_{m''} D_{m',m}^{(1/2)*} D_{m'',m}^{(1/2)} \langle pq\alpha \mathcal{J}M | (1+P)\rho^{(1)} | \Psi_{\text{He}} m' \rangle^* \langle pq\alpha \mathcal{J}M | U_\rho m'' \rangle \quad (28)$$

Since we choose the z-axis to lie in the direction \hat{Q} of the virtual photon and therefore the density operator $\rho^{(1)}$ conserves the 3N magnetic quantum number [16], one has $M = m' = m''$ and the expression Eq. (28) simplifies to

$$\begin{aligned} & D_{\frac{1}{2},m}^{(1/2)*} D_{\frac{1}{2},m}^{(1/2)} \langle pq\alpha \mathcal{J} \frac{1}{2} | (1+P)\rho^{(1)} | \Psi_{\text{He}} \frac{1}{2} \rangle \langle pq\alpha \mathcal{J} \frac{1}{2} | U_\rho \frac{1}{2} \rangle \\ & + D_{-\frac{1}{2},m}^{(1/2)*} D_{-\frac{1}{2},m}^{(1/2)} \langle pq\alpha \mathcal{J} - \frac{1}{2} | (1+P)\rho^{(1)} | \Psi_{\text{He}} - \frac{1}{2} \rangle \langle pq\alpha \mathcal{J} - \frac{1}{2} | U_\rho - \frac{1}{2} \rangle \end{aligned} \quad (29)$$

We used the fact that the $\rho^{(1)}$ matrix element is real.

Now a detailed look into the partial wave decomposed forms [16] reveals the following symmetry properties

$$\langle pq\alpha \mathcal{J} - \frac{1}{2} | (1+P)\rho^{(1)} | \Psi_{\text{He}} - \frac{1}{2} \rangle = (-1)^{\mathcal{J}-\frac{1}{2}} \Pi \langle pq\alpha \mathcal{J} \frac{1}{2} | (1+P)\rho^{(1)} | \Psi_{\text{He}} \frac{1}{2} \rangle \quad (30)$$

$$\langle pq\alpha \mathcal{J} - \frac{1}{2} | U_\rho - \frac{1}{2} \rangle = (-1)^{\mathcal{J}-\frac{1}{2}} \Pi \langle pq\alpha \mathcal{J} \frac{1}{2} | U_\rho \frac{1}{2} \rangle, \quad (31)$$

where Π is the parity of the state $|pq\alpha\rangle$. With the help of Eqs. (30-31) it is obvious that in Eq. (29) the D-functions can be separated into the sum

$$|D_{\frac{1}{2},m}^{(1/2)}|^2 + |D_{-\frac{1}{2},m}^{(1/2)}|^2 = 1 \quad (32)$$

and we end up with

$$R_L = -\frac{3}{\pi} \text{Im} \left[\sum_{\mathcal{J}} \frac{1}{E + i\epsilon - \frac{p^2}{m} - \frac{3}{4m}q^2} \langle pq\alpha \mathcal{J} \frac{1}{2} | (1+P)\rho^{(1)} | \Psi_{\text{He}} \frac{1}{2} \rangle \langle pq\alpha \mathcal{J} \frac{1}{2} | U_\rho \frac{1}{2} \rangle \right], \quad (33)$$

which is independent of m , the polarization of ${}^3\text{He}$.

A corresponding study carried through in the Appendix leads to

$$R_T = -\frac{3}{\pi} \text{Im} \left[\sum_{\mathcal{J}} \frac{1}{E + i\epsilon - \frac{p^2}{m} - \frac{3}{4m}q^2} \langle pq\alpha \mathcal{J} \frac{1}{2} | (1+P)j_1^{(1)} | \Psi_{\text{He}} - \frac{1}{2} \rangle^* \langle pq\alpha \mathcal{J} \frac{1}{2} | U_{j_1} - \frac{1}{2} \rangle \right]$$

$$+ \langle pq\alpha \mathcal{J} \frac{3}{2} | (1+P) j_1^{(1)} | \Psi_3\text{He} \frac{1}{2} \rangle^* \langle pq\alpha \mathcal{J} \frac{3}{2} | U_{j_1} \frac{1}{2} \rangle \rangle \quad (34)$$

Here $j_1^{(1)}$ is the spherical +1 component of the current operator. Again we see that R_T is independent of the ^3He target polarization.

As the second illustration we regard $R_{TL'}$. According to Eqs. (7), (22) and (26) it has the form

$$\begin{aligned} R_{TL'} &= -2 \frac{3}{2\pi} \text{Im} \left[\langle \Psi_3\text{He} | \rho^{(1)\dagger} G_0 (1+P) U_{j_1} \rangle^* - \langle \Psi_3\text{He} | j_1^{(1)\dagger} G_0 (1+P) U_\rho \rangle \right. \\ &\quad \left. + \langle \Psi_3\text{He} | \rho^{(1)\dagger} G_0 (1+P) U_{j_{-1}} \rangle^* - \langle \Psi_3\text{He} | j_{-1}^{(1)\dagger} G_0 (1+P) U_\rho \rangle \right] \\ &= -\frac{3}{\pi} \text{Im} \left[\sum_{\mathcal{J}} \frac{1}{E - i\epsilon - \frac{p^2}{m} - \frac{3}{4m} q^2} \sum_{m', m''} D_{m', m}^{(1/2)} D_{m'', m}^{(1/2)*} \langle pq\alpha | (1+P) \rho^{(1)} | \Psi_3\text{He} m' \rangle \right. \\ &\quad \left(\langle pq\alpha | U_{j_1} m'' \rangle^* + \langle pq\alpha | U_{j_{-1}} m'' \rangle^* \right) \\ &\quad - \frac{1}{E + i\epsilon - \frac{p^2}{m} - \frac{3}{4m} q^2} \sum_{m', m''} D_{m', m}^{(1/2)*} D_{m'', m}^{(1/2)} \\ &\quad \left. \left(\langle pq\alpha | (1+P) j_1^{(1)} | \Psi_3\text{He} m' \rangle^* + \langle pq\alpha | (1+P) j_{-1}^{(1)} | \Psi_3\text{He} m' \rangle^* \right) \langle pq\alpha | U_\rho m'' \rangle \right] \quad (35) \end{aligned}$$

Now j_1 (j_{-1}) increases (decreases) the magnetic quantum number by 1. Consequently

$$\begin{aligned} R_{TL'} &= -\frac{3}{\pi} \text{Im} \left[\sum_{\mathcal{J}} \frac{1}{E - i\epsilon - \frac{p^2}{m} - \frac{3}{4m} q^2} \right. \\ &\quad \left(D_{\frac{1}{2}, m}^{(1/2)} D_{-\frac{1}{2}, m}^{(1/2)*} \langle pq\alpha \mathcal{J} \frac{1}{2} | (1+P) \rho^{(1)} | \Psi_3\text{He} \frac{1}{2} \rangle \langle pq\alpha \mathcal{J} \frac{1}{2} | U_{j_1} - \frac{1}{2} \rangle^* \right. \\ &\quad \left. + D_{-\frac{1}{2}, m}^{(1/2)} D_{\frac{1}{2}, m}^{(1/2)*} \langle pq\alpha \mathcal{J} - \frac{1}{2} | (1+P) \rho^{(1)} | \Psi_3\text{He} - \frac{1}{2} \rangle \langle pq\alpha \mathcal{J} - \frac{1}{2} | U_{j_{-1}} \frac{1}{2} \rangle^* \right) \\ &\quad - \frac{1}{E + i\epsilon - \frac{p^2}{m} - \frac{3}{4m} q^2} \left(D_{-\frac{1}{2}, m}^{(1/2)*} D_{\frac{1}{2}, m}^{(1/2)} \langle pq\alpha \mathcal{J} \frac{1}{2} | (1+P) j_1^{(1)} | \Psi_3\text{He} - \frac{1}{2} \rangle^* \langle pq\alpha \mathcal{J} \frac{1}{2} | U_\rho \frac{1}{2} \rangle \right. \\ &\quad \left. + D_{\frac{1}{2}, m}^{(1/2)*} D_{-\frac{1}{2}, m}^{(1/2)} \langle pq\alpha \mathcal{J} - \frac{1}{2} | (1+P) j_{-1}^{(1)} | \Psi_3\text{He} \frac{1}{2} \rangle^* \langle pq\alpha \mathcal{J} - \frac{1}{2} | U_\rho - \frac{1}{2} \rangle \right) \left. \right] \quad (36) \end{aligned}$$

Again we use phase relations

$$\langle pq\alpha \mathcal{J} - \frac{1}{2} | (1+P) j_{-1}^{(1)} | \Psi_3\text{He} \frac{1}{2} \rangle = (-1)^{\mathcal{J}-\frac{1}{2}} \Pi \langle pq\alpha \mathcal{J} \frac{1}{2} | (1+P) j_1^{(1)} | \Psi_3\text{He} - \frac{1}{2} \rangle \quad (37)$$

$$\langle pq\alpha \mathcal{J} - \frac{1}{2} | U_\rho - \frac{1}{2} \rangle = (-1)^{\mathcal{J}-\frac{1}{2}} \Pi \langle pq\alpha \mathcal{J} \frac{1}{2} | U_\rho \frac{1}{2} \rangle \quad (38)$$

and can simplify $R_{TL'}$ as

$$R_{TL'} = -\frac{3}{\pi} \text{Im} \sum_{\mathcal{J}} \left[\frac{1}{E - i\epsilon - \frac{p^2}{m} - \frac{3}{4m} q^2} \langle pq\alpha \mathcal{J} \frac{1}{2} | (1+P) \rho^{(1)} | \Psi_3\text{He} \frac{1}{2} \rangle \right.$$

$$\begin{aligned}
& \langle pq\alpha \mathcal{J} \frac{1}{2} | U_{j_1} - \frac{1}{2} \rangle^* \left(D_{\frac{1}{2},m}^{(1/2)} D_{-\frac{1}{2},m}^{(1/2)*} + D_{-\frac{1}{2},m}^{(1/2)} D_{\frac{1}{2},m}^{(1/2)*} \right) \\
& - \frac{1}{E + i\epsilon - \frac{p^2}{m} - \frac{3}{4m}q^2} \langle pq\alpha \mathcal{J} \frac{1}{2} | (1 + P) j_1^{(1)} | \Psi_3 \text{He} - \frac{1}{2} \rangle^* \\
& \langle pq\alpha \mathcal{J} \frac{1}{2} | U_\rho \frac{1}{2} \rangle \left(D_{-\frac{1}{2},m}^{(1/2)*} D_{\frac{1}{2},m}^{(1/2)} + D_{\frac{1}{2},m}^{(1/2)*} D_{-\frac{1}{2},m}^{(1/2)} \right) \\
& = -\frac{3}{\pi} \text{Im} \sum_f \left[\frac{1}{E - i\epsilon - \frac{p^2}{m} - \frac{3}{4m}q^2} \langle pq\alpha \mathcal{J} \frac{1}{2} | (1 + P) \rho^{(1)} | \Psi_3 \text{He} \frac{1}{2} \rangle \langle pq\alpha \mathcal{J} \frac{1}{2} | U_{j_1} - \frac{1}{2} \rangle^* \right. \\
& \left. - \frac{1}{E + i\epsilon - \frac{p^2}{m} - \frac{3}{4m}q^2} \langle pq\alpha \mathcal{J} \frac{1}{2} | (1 + P) j_1^{(1)} | \Psi_3 \text{He} - \frac{1}{2} \rangle^* \langle pq\alpha \mathcal{J} \frac{1}{2} | U_\rho \frac{1}{2} \rangle \right] \\
& \left(D_{\frac{1}{2},m}^{(1/2)} D_{-\frac{1}{2},m}^{(1/2)*} + D_{-\frac{1}{2},m}^{(1/2)} D_{\frac{1}{2},m}^{(1/2)*} \right) \\
& = \pm \frac{3}{\pi} \text{Im} \sum_f \left[\frac{1}{E + i\epsilon - \frac{p^2}{m} - \frac{3}{4m}q^2} \langle pq\alpha \mathcal{J} \frac{1}{2} | (1 + P) j_1^{(1)} | \Psi_3 \text{He} - \frac{1}{2} \rangle^* \langle pq\alpha \mathcal{J} \frac{1}{2} | U_\rho \frac{1}{2} \rangle \right. \\
& \left. - \frac{1}{E - i\epsilon - \frac{p^2}{m} - \frac{3}{4m}q^2} \langle pq\alpha \mathcal{J} \frac{1}{2} | (1 + P) \rho^{(1)} | \Psi_3 \text{He} \frac{1}{2} \rangle \langle pq\alpha \mathcal{J} \frac{1}{2} | U_{j_1} - \frac{1}{2} \rangle^* \right] \sin \theta^* \cos \phi^* \quad (39)
\end{aligned}$$

where \pm refers to $m = \pm \frac{1}{2}$, respectively. As shown in the Appendix one gets similarly

$$\begin{aligned}
R_{T'} &= \pm \cos \theta^* \frac{3}{\pi} \text{Im} \sum_f \left[\frac{1}{E + i\epsilon - \frac{p^2}{m} - \frac{3}{4m}q^2} \right. \\
& \left(\langle pq\alpha \mathcal{J} \frac{1}{2} | (1 + P) j_1^{(1)} | \Psi_3 \text{He} - \frac{1}{2} \rangle^* \langle pq\alpha \mathcal{J} \frac{1}{2} | U_{j_1} - \frac{1}{2} \rangle \right. \\
& \left. \left. - \langle pq\alpha \mathcal{J} \frac{3}{2} | (1 + P) j_1^{(1)} | \Psi_3 \text{He} \frac{1}{2} \rangle^* \langle pq\alpha \mathcal{J} \frac{3}{2} | U_{j_1} \frac{1}{2} \rangle \right) \right] \quad (40)
\end{aligned}$$

The partial wave projected matrix elements are evaluated according to our standard techniques [12–16].

The only structure functions depending on θ^* and ϕ^* are

$$R_{T'} \equiv \tilde{R}_{T'} \cos \theta^* \quad (41)$$

$$R_{TL'} \equiv \tilde{R}_{TL'} \sin \theta^* \cos \phi^* \quad (42)$$

Then according to Eqs. (1) and (3) the asymmetries are

$$\begin{aligned}
A &\equiv \frac{\frac{d\sigma}{dk' dk'_0} \Big|_{h=1} - \frac{d\sigma}{dk' dk'_0} \Big|_{h=-1}}{\frac{d\sigma}{dk' dk'_0} \Big|_{h=1} + \frac{d\sigma}{dk' dk'_0} \Big|_{h=-1}} \\
&= \frac{v_{T'} \tilde{R}_{T'} \cos \theta^* + v_{TL'} \tilde{R}_{TL'} \sin \theta^* \cos \phi^*}{v_L R_L + v_T R_T} \quad (43)
\end{aligned}$$

Putting the angle θ^* between the direction of the ${}^3\text{He}$ target spin ($m = \frac{1}{2}$) and the direction \hat{Q} of the virtual photon to zero one selects the transverse asymmetry $A_{T'}$ (proportional to $\tilde{R}_{T'}$), whereas putting that angle to 90° one gets the transverse-longitudinal asymmetry $A_{TL'}$ (proportional to $\tilde{R}_{TL'}$).

Let us now regard the most simplified picture. We neglect all final state interactions, thereby excluding also the pd break up channel. Also the antisymmetrization is kept only in the two-body subsystem described by \vec{p} . Finally we restrict the ${}^3\text{He}$ wave function to the principal S-state. In order to define clearly our notation we start from the matrix elements for the symmetrized plane wave impulse approximation PWIAS

$$\begin{aligned} N_{PWIAS}^\mu &\equiv \frac{1}{\sqrt{3!}} \langle \vec{p}\vec{q}\vec{m}_1 m_2 m_3 \tau_1 \tau_2 \tau_3 | (1 - P_{23})(1 + P) j^\mu(\vec{Q}) | \Psi_{3\text{He}} m \rangle_{\theta^* \phi^*} \\ &= \frac{3}{\sqrt{3!}} \langle \vec{p}\vec{q}\vec{m}_1 m_2 m_3 \tau_1 \tau_2 \tau_3 | (1 - P_{23})(1 + P) j_{(1)}^\mu(\vec{Q}) | \Psi_{3\text{He}} m \rangle_{\theta^* \phi^*} \end{aligned} \quad (44)$$

As before we reduced the single nucleon current operator to one term. The subscript (1) indicates the particle number, which in our notation is described by \vec{q} . Now we drop the permutation operator P , apply P_{23} and insert the principal S-state approximation. The resulting nuclear matrix elements are

$$\tilde{N}_0 \equiv \sqrt{6} \langle \vec{p}\vec{q}\vec{m}_1 m_2 m_3 \tau_1 \tau_2 \tau_3 | \rho^{(1)}(\vec{Q}) | \Psi_{3\text{He}}^{PS} m \rangle_{\theta^* \phi^*} \quad (45)$$

$$\tilde{N}_\pm \equiv \sqrt{6} \langle \vec{p}\vec{q}\vec{m}_1 m_2 m_3 \tau_1 \tau_2 \tau_3 | j_\pm^{(1)}(\vec{Q}) | \Psi_{3\text{He}}^{PS} m \rangle_{\theta^* \phi^*}, \quad (46)$$

The principal S-state is

$$| \Psi_{3\text{He}}^{PS} m \rangle = | \phi_S \rangle | \xi_a m \rangle, \quad (47)$$

where $| \xi_a m \rangle$ is the totally antisymmetrical spin-isospin state

$$| \xi_a m \rangle = \frac{1}{\sqrt{2}} (| (t = 0\frac{1}{2}) T = \frac{1}{2} \rangle | (s = 1\frac{1}{2}) S = \frac{1}{2} m \rangle - | (t = 1\frac{1}{2}) T = \frac{1}{2} \rangle | (s = 0\frac{1}{2}) S = \frac{1}{2} m \rangle) \quad (48)$$

and $| \phi_S \rangle$ is the totally symmetrical space part belonging to total orbital angular momentum $L = 0$. In terms of our standard notation [18] one easily gets

$$|\Psi_{3\text{He}}^{PS} m\rangle =$$

$$\sum_{l \text{ even}} \sum_{s,t} \int dpp^2 \int dq q^2 |pq(l)0(s\frac{1}{2})S = \frac{1}{2}m(t\frac{1}{2})T = \frac{1}{2}\rangle \phi_l(pq) \frac{1}{\sqrt{2}} (\delta_{s1}\delta_{t0} - \delta_{s0}\delta_{t1}) \quad (49)$$

with

$$\phi_l(pq) = \frac{1}{\sqrt{2}} \left(\Psi_{(u)0(1\frac{1}{2})\frac{1}{2}(0\frac{1}{2})\frac{1}{2}}(pq) - \Psi_{(u)0(0\frac{1}{2})\frac{1}{2}(1\frac{1}{2})\frac{1}{2}}(pq) \right) \quad (50)$$

and $\Psi_\alpha(pq)$ are the wave function components $\langle pq\alpha|\Psi m\rangle$ determined in the Faddeev scheme.

Using (24) and (47) the nuclear matrix elements (45) and (46) turn into

$$\tilde{N}_0 = \sqrt{6}F_1^{(\tau_1)}(\vec{Q}) \sum_{m'} D_{m',m}^{(1/2)} \phi_S(\vec{p}, \vec{q} - \frac{2}{3}\vec{Q}) \langle m_1 m_2 m_3 \tau_1 \tau_2 \tau_3 | \xi_a m' \rangle \quad (51)$$

$$\begin{aligned} \tilde{N}_{\pm 1} &= \sqrt{6}F_1^{(\tau_1)}(\vec{Q}) \frac{q_{\pm 1}}{m_N} \sum_{m'} D_{m',m}^{(1/2)} \phi_S(\vec{p}, \vec{q} - \frac{2}{3}\vec{Q}) \langle m_1 m_2 m_3 \tau_1 \tau_2 \tau_3 | \xi_a m' \rangle \\ &- \sqrt{12}G_M^{(\tau_1)}(\vec{Q}) \frac{|\vec{Q}|}{2m_N} \sum_{m'} D_{m',m}^{(1/2)} \phi_S(\vec{p}, \vec{q} - \frac{2}{3}\vec{Q}) \langle m_1 \mp 1 m_2 m_3 \tau_1 \tau_2 \tau_3 | \xi_a m' \rangle \end{aligned} \quad (52)$$

Thereby the single particle current operator has been chosen according to [13]. Despite the approximate, not fully antisymmetrized final state in (45) and (46), we stick to the summation prescription over all final states in the evaluation of the structure functions, which corresponds to the fully antisymmetrized final states in Eq. (44):

$$\sum_f \equiv \frac{1}{6} \sum_{m_1 m_2 m_3} \sum_{\tau_1 \tau_2 \tau_3} \int d\vec{p} d\vec{q} \quad (53)$$

Then a straightforward evaluation yields

$$R_L = \frac{2m_N}{3} \int_0^{p_{\max}} dpp^2 q \int d\hat{p} \int d\hat{q} |\phi_S(\vec{p}, \vec{q} - \frac{2}{3}\vec{Q})|^2 \left(\frac{1}{3}(F_1^{(n)}(\vec{Q}))^2 + \frac{2}{3}(F_1^{(p)}(\vec{Q}))^2 \right) \quad (54)$$

$$R_T = \frac{2m_N}{3} \int_0^{p_{\max}} dpp^2 q \int d\hat{p} \int d\hat{q} |\phi_S(\vec{p}, \vec{q} - \frac{2}{3}\vec{Q})|^2$$

$$\left[\frac{8\pi}{9} \frac{|\vec{q}|^2}{m_N^2} |Y_{1,1}(\hat{q})|^2 \left((F_1^{(n)}(\vec{Q}))^2 + 2(F_1^{(p)}(\vec{Q}))^2 \right) + \left(\frac{2}{3}(G_M^{(n)}(\vec{Q}))^2 + \frac{4}{3}(G_M^{(p)}(\vec{Q}))^2 \right) \frac{|\vec{Q}|^2}{4m_N^2} \right] \quad (55)$$

$$R_{T'} = \frac{2m_N}{3} \int_0^{p_{\max}} dpp^2q \int d\hat{p} \int d\hat{q} |\phi_S(\vec{p}, \vec{q} - \frac{2}{3}\vec{Q})|^2 \left(-\frac{1}{6} \cos \theta^*\right) (G_M^{(n)}(\vec{Q}))^2 \frac{|\vec{Q}|^2}{m_N^2} \quad (56)$$

$$R_{TL'} = \frac{2m_N}{3} \int_0^{p_{\max}} dpp^2q \int d\hat{p} \int d\hat{q} |\phi_S(\vec{p}, \vec{q} - \frac{2}{3}\vec{Q})|^2 \frac{\sqrt{2}}{3} F_1^{(n)}(\vec{Q}) G_M^{(n)}(\vec{Q}) \frac{|\vec{Q}|}{m_N} \cos \phi^* \sin \theta^* \quad (57)$$

The energy conserving delta function gives p_{\max} and q to be

$$p_{\max} = \sqrt{m_N E} \quad (58)$$

$$q = \sqrt{\frac{4}{3}(p_{\max}^2 - p^2)}. \quad (59)$$

Note that R_L and R_T receive contributions from neutrons and protons, whereas due to the principal S-state assumption $R_{T'}$ and $R_{TL'}$ are fed only by the neutron contribution. It results in the asymmetry

$$A = \left[v_{T'} \left(-\frac{1}{6} \cos \theta^*\right) (G_M^{(n)}(\vec{Q}))^2 \frac{|\vec{Q}|^2}{m_N^2} + v_{TL'} \frac{\sqrt{2}}{3} F_1^{(n)}(\vec{Q}) G_M^{(n)}(\vec{Q}) \frac{|\vec{Q}|}{m_N} \cos \phi^* \sin \theta^* \right] \\ / \left[v_L \left(\frac{1}{3} (F_1^{(n)}(\vec{Q}))^2 + \frac{2}{3} (F_1^{(p)}(\vec{Q}))^2 \right) + \right. \\ \left. v_T \left\{ \left((F_1^{(n)}(\vec{Q}))^2 + 2(F_1^{(p)}(\vec{Q}))^2 \right) \alpha(\omega, |\vec{Q}|) + \left(\frac{2}{3} (G_M^{(n)}(\vec{Q}))^2 + \frac{4}{3} (G_M^{(p)}(\vec{Q}))^2 \right) \frac{|\vec{Q}|^2}{4m_N^2} \right\} \right], \quad (60)$$

where

$$\alpha(\omega, |\vec{Q}|) = \frac{\frac{8\pi}{9} \int_0^{p_{\max}} dpp^2q \int d\hat{p} \int d\hat{q} |\phi_S(\vec{p}, \vec{q} - \frac{2}{3}\vec{Q})|^2 \frac{|\vec{q}|^2}{m_N^2} |Y_{1,1}(\hat{q})|^2}{\int_0^{p_{\max}} dpp^2q \int d\hat{p} \int d\hat{q} |\phi_S(\vec{p}, \vec{q} - \frac{2}{3}\vec{Q})|^2} \\ = \frac{1}{3} \frac{\int_0^{p_{\max}} dpp^2q \frac{q^2}{m_N^2} \sum_l \int_{-1}^1 dx (1-x^2) \phi_l^2(p, |\vec{q} - \frac{2}{3}\vec{Q}|)}{\int_0^{p_{\max}} dpp^2q \sum_l \int_{-1}^1 dx \phi_l^2(p, |\vec{q} - \frac{2}{3}\vec{Q}|)} \quad (61)$$

with $x = \hat{q} \cdot \hat{Q}$.

That factor $\alpha(\omega, |\vec{Q}|)$ is due to the convection current, whose contribution survives solely in R_T and prevents that the dependence on the ${}^3\text{He}$ wave function drops out. It is typically

of the order 10^{-3} and together with $F_1^2(\vec{Q})$ of neutron and proton it is negligible in relation to the other term at the momentum transfer $|\vec{Q}|$ considered.

If we insert the explicit expressions for the kinematical factors v and use the nonrelativistic approximation $Q^2 \approx -\vec{Q}^2$ we get

$$A = \frac{\frac{Q^2}{2m_N^2} \tan \frac{\Theta}{2} \left[\sqrt{\frac{-Q^2}{Q^2} + \tan^2 \frac{\Theta}{2}} (G_M^{(n)})^2 \cos \theta^* + \frac{2m_N}{|\vec{Q}|} F_1^{(n)} G_M^{(n)} \cos \phi^* \sin \theta^* \right]}{(F_1^{(n)})^2 + 2(F_1^{(p)})^2 - \frac{Q^2}{4m_N^2} \left[(G_M^{(n)})^2 + 2(G_M^{(p)})^2 + \alpha \frac{6m_N^2}{|\vec{Q}|^2} \left((F_1^{(n)})^2 + 2(F_1^{(p)})^2 \right) \right]} (1 + 2 \tan^2 \frac{\Theta}{2})} \quad (62)$$

where we kept $(\frac{-Q^2}{Q^2})$ under the square root in order to facilitate the comparison to the asymmetry gained by scattering a polarized electron on a polarized nucleon target. That well known expression is

$$A_{\text{nuc}} = \frac{\frac{Q^2}{2m_N^2} \tan \frac{\Theta}{2} \left(\sqrt{\frac{-Q^2}{Q^2} + \tan^2 \frac{\Theta}{2}} G_M^2 \cos \theta^* + \frac{2m_N}{|\vec{Q}|} G_E G_M \cos \phi^* \sin \theta^* \right) \left(1 - \frac{Q^2}{4m_N^2} \right)}{G_E^2 - \frac{Q^2}{4m_N^2} G_M^2 (1 + 2(1 - \frac{Q^2}{4m_N^2})) \tan^2 \frac{\Theta}{2}} \quad (63)$$

The numerators in (62) and (63) are equal except that we use F_1 instead of G_E . Our single nucleon current operator [13] contains F_1 . In the denominator of (62), however, there are also contributions from the protons in ^3He and the correction term α resulting from the convection current. In ^3He the nucleons are moving in contrast to the case of a fixed single nucleon target.

Regarding the expression (62) we see that the transverse asymmetry $A_{T'}$ defined for $\theta^* = 0^\circ$ is proportional to $(G_M^{(n)})^2$, whereas the transverse-longitudinal asymmetry $A_{TL'}$ defined for $\theta^* = 90^\circ$ is proportional to $F_1^{(n)} G_M^{(n)}$. Will that simple result survive under more realistic conditions ?

This is just the aim of our study to learn how a more realistic ^3He wave function, the inclusion of antisymmetrization in the final state and the inclusion of final state interactions among the three final nucleons modifies that simple picture and whether these modifications will still leave sufficient sensitivity to the value of the magnetic form factor $G_M^{(n)}$ of the neutron.

Let us now define the various levels of evaluating the two asymmetries $A_{T'}$ and $A_{TL'}$. The form (62) based on the principal S-state and plane wave impulse approximation without

antisymmetrization in the final state (see Eqs. (45)–(46)) will be denoted by PWIA (PS). If we include the realistic ^3He wave function we denote the result by PWIA. The corresponding structure functions are determined by (22) dropping the factor 3, the permutation operator P and U_B and U_A should be chosen by (19) without the two terms proportional to the NN t-matrix t . If one restricts $|\Psi_{^3\text{He}}\rangle$ to the principal S-state the results should be identical to the structure functions evaluated according to Eqs. (54)–(57) and to the asymmetry from (62). This is a very nontrivial check and turned out to be very well fulfilled.

The next improvement of the theory is to keep plane waves in the final state but antisymmetrize them correctly. This is achieved using (22) and dropping only in the U -amplitudes of Eq. (19) the terms proportional to t . This approximation will be denoted by PWIAS.

An intermediate step for including the full final state interaction is to keep in the nuclear matrix elements the interaction in the pair of nucleons which are spectators to the absorption process of the photon on the third nucleon. This approximation is described by the nuclear matrix elements

$$N_0' = \sqrt{6} \langle \vec{p}\vec{q}m'_1m'_2m'_3 | (1 + tG_0)\rho^{(1)}(\vec{Q}) | \Psi_{^3\text{He}}m \rangle_{\theta^*\phi^*} \quad (64)$$

$$N_{\pm}' = \sqrt{6} \langle \vec{p}\vec{q}m'_1m'_2m'_3 | (1 + tG_0)j_{\pm}^{(1)}(\vec{Q}) | \Psi_{^3\text{He}}m \rangle_{\theta^*\phi^*} \quad (65)$$

for the ppn-breakup process and by

$$N_{0,d}' = \langle \varphi_d \vec{q}m'_1m'_d | \rho^{(1)}(\vec{Q}) | \Psi_{^3\text{He}}m \rangle_{\theta^*\phi^*} \quad (66)$$

$$N_{\pm 1,d}' = \langle \varphi_d \vec{q}m'_1m'_d | j_{\pm}^{(1)}(\vec{Q}) | \Psi_{^3\text{He}}m \rangle_{\theta^*\phi^*} \quad (67)$$

for the pd-breakup process. Note that we did not antisymmetrize the final state except in the two-body subsystem. This leads to the expression (22) without the factor 3 and the permutation operator P , and the U -amplitudes are just given by the driving term in Eq. (19). The corresponding results will be denoted by PWIA'. If on top of that we antisymmetrize the final state the result will be denoted by PWIAS'. This is evaluated using Eq. (22) as it is, but the U -amplitude as for PWIA'.

Finally evaluating (22) and (19) exactly and thus including the final state interaction to all orders and between all three nucleons, as well as including the antisymmetrization fully will be denoted by FULL.

III. RESULTS

We used the Bonn B NN potential [19] and kept its force components up to total two-nucleon angular momentum $j=2$ in the treatment of the 3N continuum. The effects of the $j=3$ components stayed below the percentage level. The electromagnetic nucleon form factors are from [20].

The experimental setup for the spin-dependent asymmetry can be characterized by the initial electron energy (k_0), the electron scattering angle (Θ), two angles which parametrize the direction of the target polarization (θ_A, ϕ_A) (see Fig. 7 of Ref. [10], e.g.), and the measured energy transfer (ω). These values used in the recent experiments [7–9] are summarized in Table I, together with energy transfer (ω_{QE}), 3-momentum transfer ($|\vec{Q}|_{QE}$) and the angles defining the polarization with respect to the direction \hat{Q} of the 3-momentum transfer (θ_{QE}^* and ϕ_{QE}^*) at the quasielastic (QE) condition. The asymmetry measured in Ref. [7] near the quasielastic kinematics is essentially the transverse asymmetry $A_{T'}$ because of the condition, $\theta^* \simeq 0^\circ$, and then is expected to be sensitive to the neutron magnetic form factor. Thus hereafter the asymmetry measured in this experiment will be referred to as simply $A_{T'}$. On the other hand, those measured near the quasielastic kinematics [8] and a lower- ω region just above the 3-body breakup threshold [9] are essentially the transverse-longitudinal asymmetry $A_{TL'}$ because of the condition, $\theta^* \simeq 90^\circ$, and then are expected to be sensitive to both of the neutron charge and magnetic form factors. Hereafter the asymmetry measured in these experiments will be referred to as simply $A_{TL'}$. These experimental results were analyzed by recent theoretical works [10,11] with realistic ^3He wave functions and plane wave impulse approximation. In this article we call that approximation PWIA'. In Ref. [7], the neutron magnetic form factor, G_M^n , was extracted based on PWIA' with reasonable agreement with

experimental data. On the other hand, agreement between the PWIA' calculations and the measured asymmetries in Refs. [8,9] is rather poor. The PWIA' prediction of the asymmetry in the quasielastic region was found to be large compared to the experimental data [8] at the $(1 - 2.5)\sigma$ level. At the lower ω -region [9], the experimental asymmetry was found to be enhanced in contradiction with PWIA' calculations.

Let us now regard our results in comparison to the experimental data for $A_{T'}$ in Fig. 1 and for $A_{TL'}$ in Fig. 2. We display six theoretical curves. The most naive prediction, PWIA(PS) lies within the error bars for four of the six data points for $A_{T'}$ in Fig. 1. In case of $A_{TL'}$ shown in Fig. 2 that prediction is essentially zero and clearly disagrees with the data. Replacing the principal S-state approximation of ${}^3\text{He}$ by the full expression, called PWIA, causes a visible change for $A_{T'}$ at low ω 's and a much larger one for $A_{TL'}$. Now for $A_{TL'}$ one deviates even stronger from the data. Apparently $R_{TL'}$ is more sensitive to the ${}^3\text{He}$ wave function than $R_{T'}$. Symmetrizing the final state using PWIAS has a small effect for $A_{T'}$ but a big one on $A_{TL'}$. It rises $A_{TL'}$ for small ω 's qualitatively similar to what happens in the data but misses the data around $\omega = 60\text{--}70$ MeV. A strong move occurs by keeping the final state interaction among the two spectator nucleons, PWIA'. For lower ω 's it appears to be somewhat too high for $A_{T'}$ and again at low ω 's near the threshold for 3N breakup it does not show the quick rise of the one data point in $A_{TL'}$. However between 50 and 100 MeV it follows the data for $A_{TL'}$. Now symmetrizing in addition the final state, PWIAS', it does not cause a visible change for $A_{T'}$, but overshoots now the data for $A_{TL'}$ for ω 's below about 70 MeV. Finally the full calculation leads again to a strong shift and agrees now quite well with the data for both $A_{T'}$ and $A_{TL'}$. At very low ω 's it now follows the experimental trend for $A_{TL'}$ though still misses the error bar of the last data point to the left. More precise data for $A_{TL'}$, especially in that region would be of interest to quantitatively challenge our present day understanding of final state interactions but possibly also effects related to the choice of the current operator.

Though the data show still some scatter for $A_{T'}$ we would like to quantify these results by providing a χ^2 for $A_{T'}$:

$$\chi^2 \equiv \sum_i \frac{(A_{T'}^{\text{theory}}(i) - A_{T'}^{\text{exp}}(i))^2}{(A_{T'}^{\text{exp}}(i))^2} \quad (68)$$

The sum runs over the six data points. They are 4.2, 4.1, 4.0, 6.1, 6.3, 3.4 for PWIA(PS), PWIA, PWIAS, PWIA', PWIAS' and FULL, respectively. The FULL calculation describes the data best and the correct antisymmetrization and the treatment of the full final state interaction is required to achieve quantitative insight. Note that the often used plane wave impulse approximation, here called PWIA' is insufficient.

The aim of the experiments were to achieve information on the magnetic neutron form factor. Therefore the influence of the badly known electric form factor of the neutron, $G_E^{(n)}$, or in our nonrelativistic form $F_1^{(n)}$ should be known. We restrict our investigation to $A_{T'}$ and in addition to PWIA(PS) and PWIAS. As an extreme assumption we put $F_1^{(n)}$ to zero, the effect on $A_{T'}$ was negligible (below 1 %). We expect that this remains true even for the FULL calculation and therefore we expect that the specific choice of $F_1^{(n)}$ will not influence significantly the extraction of information on $G_M^{(n)}$ from $A_{T'}$.

We add the remark that this extreme assumption puts $A_{TL'} = 0$ for PWIA(PS), of course. Obviously the data are different from zero and $A_{TL'}$ receives contributions from ingredients, which go beyond that most simplistic picture. This can already be seen comparing PWIA(PS) and PWIA in Fig. 2. The difference is just the replacement of the principal S-state ^3He wave function by the realistic one. Apparently the S'- and D-state pieces contribute very strongly to $A_{TL'}$. This was noticed before in [10].

Being free of that dependence on $F_1^{(n)}$ for $A_{T'}$, we now altered the neutron magnetic form factor by $\pm 15\%$ and $\pm 30\%$ and achieved the results, for the FULL calculation displayed in Fig. 3. Clearly $\pm 30\%$ changes lie outside the bulk of the data and also $\pm 15\%$ changes are not acceptable given the data. One can quantify these studies and extract the optimal f factor multiplying the neutron magnetic form factor $G_M^{(n)}$ of [20] such that χ^2 is minimal. This study was performed for the FULL calculation. We display the resulting χ^2 in Fig. 4 and extract the optimal f factor to be 1. As a measure of the accuracy of extracting that value we take the spread in f for $\chi_{\text{min}}^2 + 1$. This is $\pm 6.6\%$. Clearly more precise data would

be very welcome to improve on the accuracy of extracting information on $G_M^{(n)}$.

The possibly most serious theoretical uncertainty in our analysis is that we do not take MEC s into account. Their quantitative contribution remains to be investigated. It also remains to be seen whether different choices of NN forces could change the results. For inclusive scattering without polarisation we found only a very weak dependence [16]. Simplified calculations keeping only $j_{\max} = 1$ NN force components, now for the polarization case, also did not show a dependence on the choice of the NN force.

For future experimental work we would like to propose to separate $R_{T'}$ and $R_{TL'}$. The sensitivity of $R_{T'}$ to $G_M^{(n)}$ is larger than for the asymmetry $A_{T'}$. This is demonstrated in Fig. 5 in comparison to Fig. 3 again for the FULL calculation. Again we quantify that study by evaluating a χ^2 , defined now as

$$\chi^2(R_{T'}, A_{T'}) \equiv \sum_i \frac{\left(R_{T'}^{(i)}(A_{T'}^{(i)})(f = 1) - R_{T'}^{(i)}(A_{T'}^{(i)})(f = 1.3) \right)^2}{\left(R_{T'}^{(i)}(A_{T'}^{(i)})(f = 1) \right)^2}, \quad (69)$$

where i runs over the ω -values, in which we carried out the calculations. We find $\chi^2(R_{T'}) = 3.1$ and $\chi^2(A_{T'}) = 2.3$. Thus $R_{T'}$ has a stronger dependence on the magnetic neutron form factor (modified by the strength factor f) than $A_{T'}$. For the sake of curiosity Fig.5 also includes the results putting $G_M^{(n)} = 0$ ($f=0$).

IV. SUMMARY

Inclusive scattering of polarised electrons on polarised ${}^3\text{He}$ has been evaluated taking the final state interaction fully into account. Realistic NN forces have been used and the 3N bound state and the 3N continuum are evaluated consistently solving the corresponding Faddeev equations. A formalism proposed in [14], which is ideal for inclusive processes and avoids the tedious direct integration of over all final state configurations, has been generalized to handle new types of structure functions composed of different current components.

The most simple picture of polarized ${}^3\text{He}$ to be a polarized neutron target fails quantitatively for the energy and momentum transfers considered. That picture relies on the

assumption, that the principal S-state is by far dominant. This is not at all true for the transverse- longitudinal asymmetry $A_{TL'}$, which receives important contributions from the remaining pieces of the ^3He wave function, but also for the transverse asymmetry $A_{T'}$, where the results change significantly when the principal S-state approximation is replaced by the full and correct ^3He wave function.

We also find that the often used plane - wave impulse approximation (here denoted by PWIA') is insufficient. In PWIA' one takes the NN force in the final state into account for the pair of nucleons which are spectators to the single nucleon photon absorption of the third nucleon. This is quite insufficient for $A_{T'}$ and $A_{TL'}$. The correct antisymmetrization of the final 3N continuum is important and above all the final state interaction only all three nucleons (FULL calculation).

In the FULL calculation the data for $A_{T'}$ can be described quite well using the Gari-Krümpelmann electromagnetic nucleon form factors. The dependence of that observable $A_{T'}$ on the neutron F_1 form factor is weak and unimportant. We optimized the choice of $G_M^{(n)}$ to the data, with the result that the factor $f=1$ for the choice of Gari-Krümpelmann parametrization was best. This appears to agree with preliminary results achieved in electron scattering on the deuteron [21].

In the case of $A_{TL'}$ the FULL calculation shows now the enhancement near the 3N breakup threshold, which is present in the data and which was not provided by the plane wave impulse approximation used up to now.

For both observables $A_{T'}$ and $A_{TL'}$ more precise data would be very welcome in order to probe the theoretical assumptions more stringently and to extract more accurate information on $G_M^{(n)}$.

A more thorough investigation of $A_{TL'}$ with respect to the contribution of the proton and the ^3He wave function component is planned. Because of lack of computer time it could not be included in this study.

We would also like to point out that data for $R_{T'}$ and $R_{TL'}$ would be more sensitive to electromagnetic nucleon form factors than the asymmetries. From the theoretical point of

view mesonic exchange currents should be added and the treatment of relativity remains a pending problem.

ACKNOWLEDGMENTS

The authors are indebted to Dr. H. Gao and Dr. C. E. Jones for providing the details of their data. This work was supported by the Polish Committee for Scientific Research under Grant PB 1031 and the Science and Technology Cooperation Germany-Poland under Grant No. XO81.91. The numerical calculations have been performed on the Cray T90 of the Höchstleistungsrechenzentrum in Jülich, Germany.

REFERENCES

- [1] R. G. Arnold *et al.*, Phys. Rev. Lett. **57** (1986) 174; P. E. Bosted *et al.*, Phys. Rev. Lett. **68** (1992) 3841.
- [2] P. Markowitz *et al.*, Phys. Rev. **C48** (1993) R5; J. Jourdan, AIP Conference Proceedings 334, Few-Body Problems in Physics, ed. F. Gross, Williamsburg 1994, page 339; Proceeding of the 14th International Conference on Particles and Nuclei, eds. G. E. Carlson, J.J. Domingo, Williamsburg 1996 (World Scientific 1997), page 262.
- [3] B. Blankleider, R. M. Woloshyn, Phys. Rev. **C29** (1984) 538.
- [4] J. L. Friar, B. F. Gibson, G. L. Payne, A. M. Bernstein, T. E. Chupp, Phys. Rev. **C42** (1990) 2310.
- [5] C. E. Woodward *et al.*, Phys. Rev. Lett. **65** (1990) 698; C. E. Jones-Woodward *et al.*, Phys. Rev. **C44** (1991) R571; C. E. Jones *et al.*, Phys. Rev. **C47** (1993) 110.
- [6] A. K. Thompson *et al.*, Phys. Rev. Lett. **68** (1992) 2901.
- [7] H. Gao *et al.*, Phys. Rev. **C50** (1994) R546.
- [8] J.-O. Hansen *et al.*, Phys. Rev. Lett. **74** (1995) 654.
- [9] C. E. Jones *et al.*, Phys. Rev. C **52** (1995) 1520.
- [10] R.-W. Schulze and P. U. Sauer, Phys. Rev. **C48** (1993) 38.
- [11] C. Ciofi degli Atti, E. Pace and G. Salmé, Phys. Rev. **C51** (1995) 1108.
- [12] H. Kamada, W. Glöckle, J. Golak, Nuovo Cimento **105A** (1992) 1435.
- [13] S. Ishikawa, H. Kamada, W. Glöckle, J. Golak, H. Witała, Nuovo Cimento **107A** (1994) 305.
- [14] S. Ishikawa, H. Kamada, W. Glöckle, J. Golak and H. Witała, Phys. Lett. **B339** (1994) 293.

- [15] J. Golak, H. Kamada, H. Witała, W. Glöckle, S. Ishikawa, Phys. Rev. **C51** (1995) 1638.
- [16] J. Golak, H. Witała, H. Kamada, D. Hüber, S. Ishikawa, W. Glöckle, Phys. Rev. **C52** (1995) 1216.
- [17] T. W. Donnelly and A. S. Raskin, Ann. Phys. (N.Y.) **169** (1986) 247.
- [18] W. Glöckle, *The Quantum Mechanical Few-Body Problem* (Springer-Verlag, Berlin Heidelberg New York Tokyo 1983).
- [19] R. Machleidt, Advances in Nucl. Phys. **19** (1989) 189.
- [20] M. Gari and W. Krümpelmann, Phys. Lett. **173B** (1986) 10.
- [21] J. Jourdan (private communication)

V. APPENDIX

The structure function R_T has the form

$$R_T = \sum_{m'\tau'} \int df' \delta(M + \omega - P'_0) (|N_1|^2 + |N_{-1}|^2) \quad (70)$$

Using (11) and (22) one can write

$$\begin{aligned} R_T &= -\frac{3}{\pi} \text{Im} \langle \Psi_3 \text{He} | j_1^{(1)\dagger} G_0 (1 + P) | U_{j_1}^{(1)} \rangle - \frac{3}{\pi} \text{Im} \langle \Psi_3 \text{He} | j_{-1}^{(1)\dagger} G_0 (1 + P) | U_{j_{-1}}^{(1)} \rangle \\ &= -\frac{3}{\pi} \text{Im} \left[\sum_f \frac{1}{E + i\epsilon - \frac{p^2}{m} - \frac{3}{4m} q^2} \sum_{m'} \sum_{m''} \right. \\ &\quad \left. D_{m',m}^{(1/2)*} D_{m'',m}^{(1/2)} \langle pq\alpha | (1 + P) j_1^{(1)} | \Psi_3 \text{He } m' \rangle^* \langle pq\alpha | U_{j_1}^{(1)} m'' \rangle \right] \\ &\quad - \frac{3}{\pi} \text{Im} \left[\sum_f \frac{1}{E + i\epsilon - \frac{p^2}{m} - \frac{3}{4m} q^2} \sum_{m'} \sum_{m''} \right. \\ &\quad \left. D_{m',m}^{(1/2)*} D_{m'',m}^{(1/2)} \langle pq\alpha | (1 + P) j_{-1}^{(1)} | \Psi_3 \text{He } m' \rangle^* \langle pq\alpha | U_{j_{-1}}^{(1)} m'' \rangle \right] \end{aligned} \quad (71)$$

Since $j_1^{(1)}$ ($j_{-1}^{(1)}$) increases (decreases) the m magnetic quantum by 1 one gets

$$\begin{aligned} R_T &= -\frac{3}{\pi} \text{Im} \sum_f \frac{1}{E + i\epsilon - \frac{p^2}{m} - \frac{3}{4m} q^2} [|D_{\frac{1}{2}m}|^2 \langle pq\alpha \mathcal{J} \frac{3}{2} | (1 + P) j_1^{(1)} | \Psi_3 \text{He } \frac{1}{2} \rangle^* \langle pq\mathcal{J} \frac{3}{2} | U_{j_1}^{(1)} \frac{1}{2} \rangle \\ &\quad + |D_{-\frac{1}{2}m}|^2 \langle pq\alpha \mathcal{J} \frac{1}{2} | (1 + P) j_1^{(1)} | \Psi_3 \text{He } -\frac{1}{2} \rangle^* \langle pq\mathcal{J} \frac{1}{2} | U_{j_1}^{(1)} -\frac{1}{2} \rangle] \end{aligned}$$

$$\begin{aligned}
& -\frac{3}{\pi} \text{Im} \sum_{\mathcal{J}} \frac{1}{E + i\epsilon - \frac{p^2}{m} - \frac{3}{4m} q^2} [|D_{\frac{1}{2}m}|^2 \langle pq\alpha \mathcal{J} - \frac{1}{2} | (1+P) j_{-1}^{(1)} | \Psi_{\text{He}} \frac{1}{2} \rangle^* \langle pq\mathcal{J} - \frac{1}{2} | U_{j_{-1}}^{(1)} \frac{1}{2} \rangle \\
& + |D_{-\frac{1}{2}m}|^2 \langle pq\alpha \mathcal{J} - \frac{3}{2} | (1+P) j_{-1}^{(1)} | \Psi_{\text{He}} - \frac{1}{2} \rangle^* \langle pq\mathcal{J} - \frac{3}{2} | U_{j_{-1}}^{(1)} - \frac{1}{2} \rangle] \quad (72)
\end{aligned}$$

Using the phase relation (37), in addition

$$\langle pq\alpha - \frac{3}{2} | (1+P) j_{-1}^{(1)} | \Psi_{\text{He}} - \frac{1}{2} \rangle = (-)^{\mathcal{J} - \frac{1}{2}} \Pi < pq\alpha \mathcal{J} \frac{3}{2} | (1+P) j_1^{(1)} | \Psi_{\text{He}} \frac{1}{2} \rangle \quad (73)$$

and corresponding ones for $\langle pq\alpha \mathcal{J} - \frac{1}{2} | U_{j_{-1}}^{(1)} \frac{1}{2} \rangle$ and $\langle pq\alpha \mathcal{J} - \frac{3}{2} | U_{j_{-1}}^{(1)} - \frac{1}{2} \rangle$ one arrives at (34).

The structure function $R_{T'}$ has the form

$$R_{T'} = \sum_{m'\tau'} \int df' \delta(M + \omega - P'_0) (|N_1|^2 - |N_{-1}|^2) \quad (74)$$

A corresponding manipulation as above yields

$$\begin{aligned}
R_{T'} &= -\frac{3}{\pi} \text{Im} \sum_{\mathcal{J}} \frac{1}{E + i\epsilon - \frac{p^2}{m} - \frac{3}{4m} q^2} \\
& \quad [\langle pq\alpha \mathcal{J} \frac{3}{2} | (1+P) j_1^{(1)} | \Psi_{\text{He}} \frac{1}{2} \rangle^* \langle pq\alpha \mathcal{J} \frac{3}{2} | U_{j_1}^{(1)} \frac{1}{2} \rangle (|D_{\frac{1}{2}m}|^2 - |D_{-\frac{1}{2}m}|^2) \\
& \quad + \langle pq\alpha \mathcal{J} \frac{1}{2} | (1+P) j_1^{(1)} | \Psi_{\text{He}} - \frac{1}{2} \rangle^* \langle pq\alpha \mathcal{J} \frac{1}{2} | U_{j_1}^{(1)} - \frac{1}{2} \rangle (|D_{-\frac{1}{2}m}|^2 - |D_{\frac{1}{2}m}|^2)] \quad (75)
\end{aligned}$$

Using (25) one ends up with (40).

FIGURES

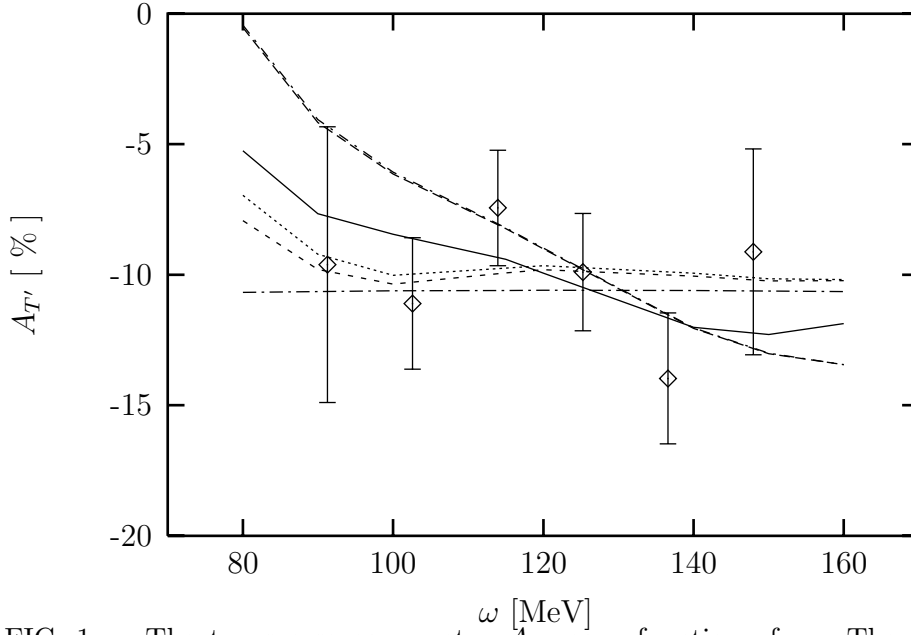


FIG. 1. The transverse asymmetry $A_{T'}$ as a function of ω . The data are from Ref [7]. The six theoretical curves are PWIA(PS)(dashed-dotted), PWIA(dotted), PWIAS(short dashed), PWIA'(long dashed), PWIAS'(dashed-dotted, declined curve) and FULL (solid). Note PWIA' and PWIAS' overlap.

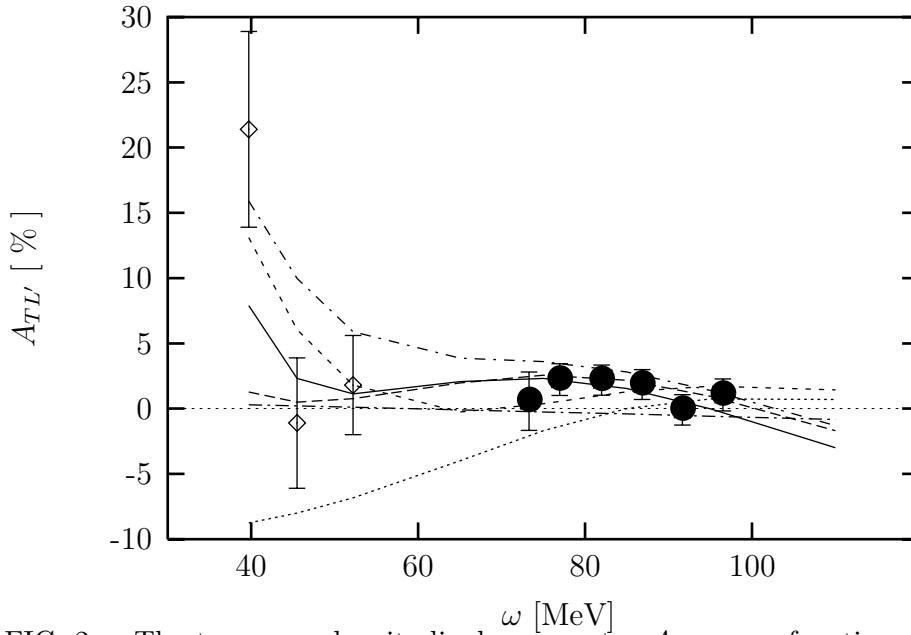


FIG. 2. The transverse-longitudinal asymmetry $A_{TL'}$ as a function of ω . The data (\diamond) are from Ref [8] and the data (\bullet) from Ref [9]. Curves as in Fig 1. The PWIAS'-curve rises to the data point at $\omega=40\text{MeV}$.

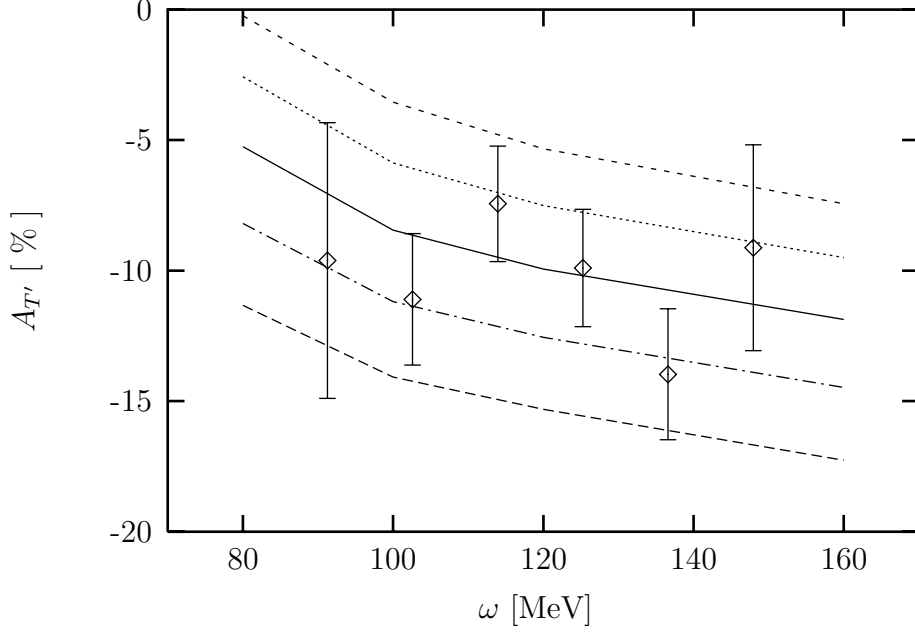


FIG. 3. The dependence of the transverse asymmetry $A_{T'}$ in the FULL calculation on the strength factor f multiplied to the neutron magnetic form factor $G_M^{(n)}$ from [20]. $f=0.7$ (short-dashed), $f=0.85$ (dotted), $f=1$ (solid), $f=1.15$ (dashed-dotted) and $f=1.3$ (long-dashed). Comparison to data from [7].

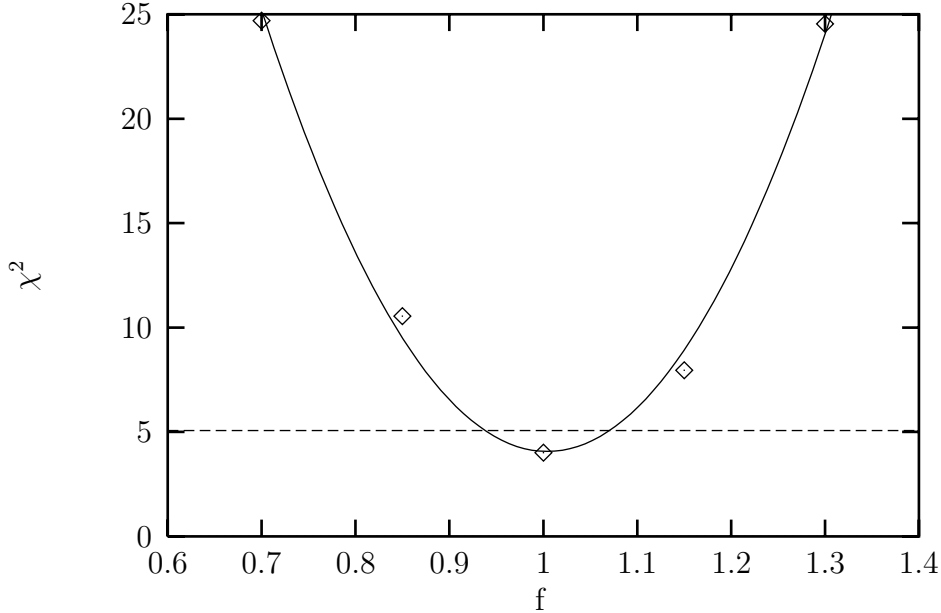


FIG. 4. The χ^2 from Eq(68) for $A_{T'}$ as a function of the strength factor f from Fig. 3. A parabola is fitted to the calculated values denoted by (\diamond). The value $\chi^2_{min} + 1$ is shown as dashed horizontal line and provides a spread of $\Delta f = \pm 6.6\%$.

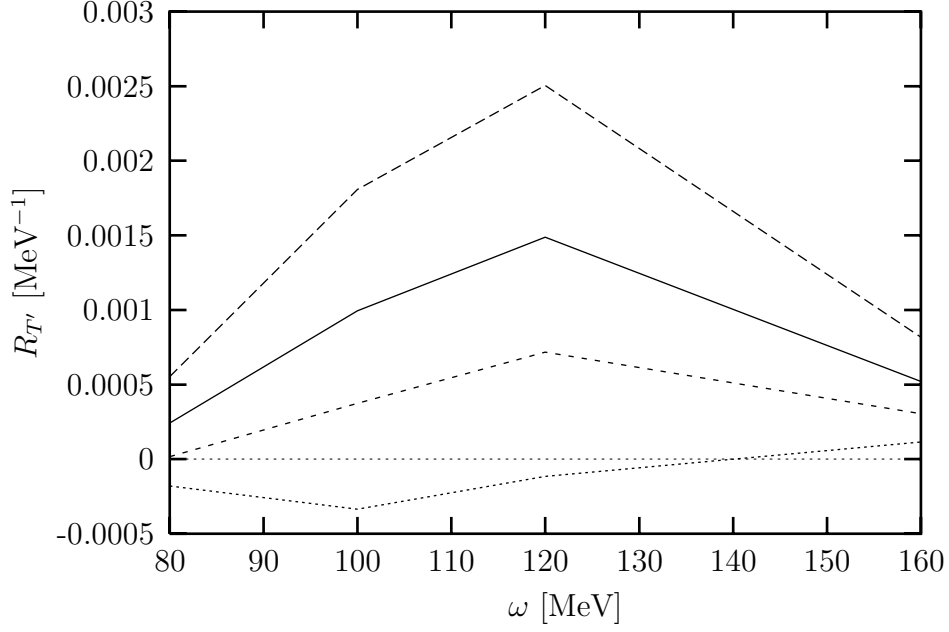


FIG. 5. The transversal structure function $R_{T'}$ as a function of ω in the FULL calculation for various strength factors f : $f=1.3$ (long dashed), $f=1$ (solid), $f=0.7$ (short dashed) and $f=0$ (dotted).

TABLES

TABLE I. The experimental setup of Refs. [7–9].

	k_0	Θ	θ_A	ϕ_A	ω	ω_{QE}	Q_{QE}	θ_{QE}^*	ϕ_{QE}^*
	(MeV)	($^\circ$)	($^\circ$)	($^\circ$)	(MeV)	(MeV)	(MeV/c)	($^\circ$)	($^\circ$)
Ref. [7]	370	91.4	42.5	180	91 – 150	107	460	8.9	180
Ref. [8]	370	70.1	42.5	0	73 – 97	76	386	88.1	0
Ref. [9]	370	70.1	42.5	0	40 – 52	76	386	88.1	0